ChemComm

Accepted Manuscript

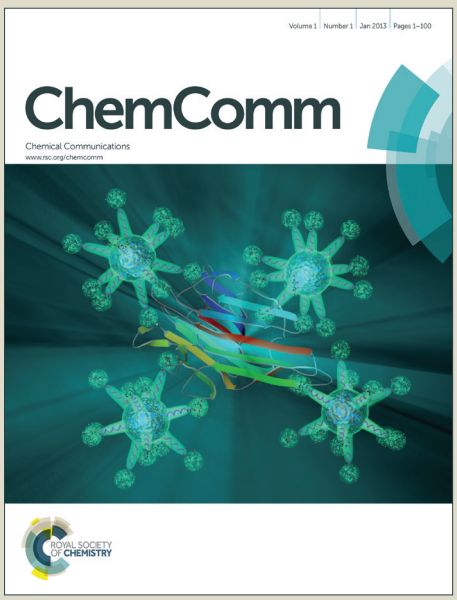

ROYAL SOCIETY OF CHEMISTRY

www.rsc.org/chemcomm

Journal Name

RSCPublishing

COMMUNICATION

Three-dimensionalization of ultrathin nanosheets in a two-dimensional nano-reactor: macroporous CuO microstructures with enhanced cycling performance

Cite this: DOI: 10.1039/x0xx00000x

Chuan-Yin Jin,[a] Ming Hu,[a] Xun-Liang Cheng,[a] Fan-Xing Bu,[a] Li Xu,[a] Qing-Hong Zhang[b] and Ji-Sen Jiang*[a]

Received ooth January 2012,
Accepted ooth January 2012

DOI: 10.1039/x0xx00000x

www.rsc.org/

Three-dimensional (3D) macroporous CuO structures composed of ultrathin nanosheets were successfully synthesized by employing a liquid-liquid interface as a two-dimensional (2D) nano-reactor. The macroporous structure helped CuO to retain the exposed surface during reactions, thus significantly enhanced the long term cycling performance both in photocatalysis and lithium ion battery.

Since the discovery of graphene,[1,2] two-dimensional ultrathin nanosheets/flakes have attracted great interests owing to the excellent size-/shape dependent property of nanosheets.[3] Because of the large specific surface area and exposed surfaces,[4] ultrathin nanosheets can interact with active species very well, or allow the insertion of external ions efficiently.[4a, 5] Such superiorities make the nanosheets to be great candidates in applications such as hetero-catalysis and energy storage. [6]

Copper oxide (CuO) has been widely utilized in various applications such as photocatalysis,[7] adsorption,[8] gas sensing[9] and lithium ions battery[10]. In recent years, CuO nanosheets have been synthesized, and showed enhanced performance in photocatalysis[11] and electrochemical application.[12] However, two main problems exist currently. Firstly, the CuO nanosheets are generally thicker than 20 nm, indicating that the nanosheets contain too many layers. Thick nanosheets have longer diffusion pathway perpendicular to the facet, and smaller accessible surface area, thus weaken the performance of CuO nanosheets in catalysis or energy storage. Secondly, agglomeration of nanosheets is hard to be avoided. The agglomeration causes the nanosheets to stack on each other seriously, reduces the chance of external species to interact with nanosheets, leading to low catalytic activity, or poor cycling capability.

To solve the problems, it is important to find a way to synthesize ultra-thin CuO nanosheets and organize them into a three-dimensional (3D) structure.[13] Three-dimensionalization was considered to be an efficient way to improve the performance of nanosheets in applications. For example, Worsley *et al.*[13a] synthesized sp^2-cross-linked three-dimensional graphene monoliths with high surface area, which exhibited extraordinarily high surface area and large pore volume, while maintaining the high conductivity observed in the resorcinol formaldehyde-derived graphene aerogels. Chen *et al*.[13b] reported a direct synthesis of 3D foam-like graphene macrostructures, which showed high electrical conductivity. In these cases, the nanosheets were well-supported, and large fraction of the surface of nanosheets was exposed, thus good physicochemical property of the material could be well maintained. Yin *et al.* synthesized 3D nanosheet-based flocculus-like hierarchical CuO nanostructures in solution, the thickness of the nanosheet were approximately 88.7 nm and 240 nm. [14]

Herein, we utilized a confined 2D space, the interface between immiscible liquids, as a nano-reactor. The nano-reactor could work as a template to confine the thickness of nanosheets. Moreover, we deduced that the obtained nanosheets could self-assemble in a 3D way in such confined space. We expected 3D ultra-thin CuO nanosheets could show superior long-term activity over either commercial CuO or non-organized nanosheets in hetero-catalysis as well as electrochemical energy storage.

In a typical procedure, a liquid interface reactor was established by placing water above hydrophobic liquid, dichloromethane, as shown in Scheme 1. The height of the reactor is estimated to be about 1nm.[15] As shown in Scheme 1a, cupric acetylacetonate was dissolved in dichloromethane phase, while sodium hydroxide was dissolved in water phase. Then, the reaction between cupric ions and hydroxide ions was forced to be within the liquid-liquid interface which also meant that the generation of CuO was confined in this limited space. Digital photos taken from the reaction system before and after reaction were shown in Scheme 1b. The black area in the

right side of Scheme 1b illustrated the formation of CuO inside the liquid-liquid interface. As the thicknesses of the interfaces can be modulated by using different types of solvents, or by changing the temperature of reaction system,[16] such approach may open a general way to prepare 3D structures composed of ultrathin nanosheets with different thickness.

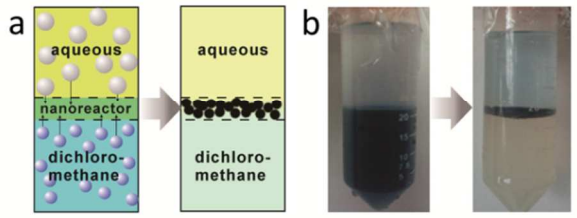

Scheme 1. (a) Scheme of the 2D nano-reactor established at the interface of immiscible liquids; (b) Photo of the reaction system before and after reaction.

Fig.S1 shows the XRD pattern of the as-prepared sample. All the peaks can be assigned as monoclinic CuO (JCPDS file no. 48-1548, space group *C2/c*). No additional peak was detected, suggesting the purity of as-prepared CuO sample. Fig. 1a is SEM image of the as-prepared CuO product, from which numerous 3D flower-like macroporous spheres were clearly observed. These structures are of a mean size of around 7-8 μm. Low-magnified FESEM image (Fig. S2) clearly reveals high yield of the 3D flower-like macroporous spheres. Fig. 1b shows the 3D structures are build up by nanosheets. The nanosheets are organized together, and support each other with almost all the surfaces exposed. The mean thickness of these nanosheets building blocks is of $6.42^{\pm}1.05$ nm (Fig. S3) according to the SEM image, which are much thinner than previous reports[17] (Table. S1). SEM image shown in Fig. 1c indicates an individual microstructure is relatively robust after the sample preparation procedure. The pore size of the structure is between 100 and 400 nm. Fig. 1d is the TEM image of a non-organized nanosheet from the broken structures. The corner of the nanosheet contains some whiskers (inside the circle in Fig. 1d), suggesting that the nanosheets may be assembled by nanowires. The corresponding SAED pattern(Fig. 3d inset) of the nanosheet is constituted of periodic spots, indicating the nanosheet is single crystalline. The projection can be indexed to [11–1] zone axis, indicating the exposed surface is (11–1).

Nitrogen sorption analysis was performed to investigate the specific surface area and porosity of such 3D macroporous CuO structures (Fig. S4). Brunauer–Emmett–Teller (BET) surface area of the 3D macroporous CuO structures was calculated to be 14 m^2g^{-1} based on the desorption curve. The hysteresis loop from P/P_0=0.6 to P/P_0=1 suggests the existence of macroporous, which is in consistence with the shape of 3D CuO nanosheets observed by SEM.

Time-dependent experiment illustrates that the generation of 3D macroporous CuO structures is a multiple-step process, from $Cu(OH)_2$ nanorods to 3D CuO structures. Fig. S5 and Fig. S6 present the XRD profiles and SEM images of the samples taken at different reaction periods, respectively. $Cu(OH)_2$ nanorods were generated at 15 min, while minor amount of CuO co-existed. After two hours, the nanorods aggregated together, and the main composition was $Cu(OH)_2$ still. The morphology of sample changed significantly when the reaction time was 6 h.

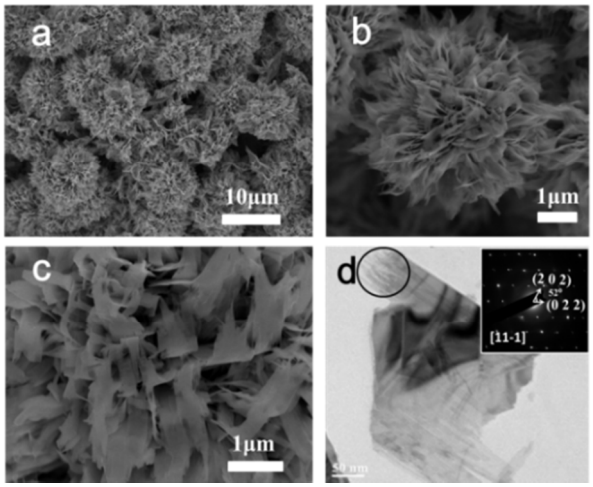

Fig. 1 Electron microscopy characterization of as-synthesized CuO sample. (a) Low-magnification SEM image of the prepared 3D macroporous CuO structure; (b) SEM image of an individual 3D macroporous CuO structure; (c) Part of an 3D macroporous CuO structure; (d) TEM image of an individual nanosheet, and the inset is the corresponding SAED pattern.

The 3D macroporous CuO structures became the main product, while more CuO was generated. When the time reached to 10 h, $Cu(OH)_2$ dismissed, while CuO was the only product. The 3D macroporous CuO structures formed from 6 h was retained after 12 h as shown in Fig. S6c and Fig. S6d.

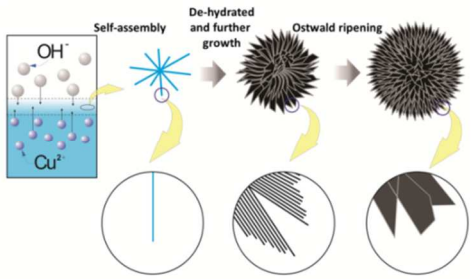

Fig. 2 Possible formation process of obtained 3D macroporous CuO structures composed of nanosheets.

On the basis of above multiple-step process, possible mechanism was proposed as shown in Fig. 2. From the very beginning of reaction, hydroxide ions in water phase reacted with $Cu(acac)_2$ in oil phase at the liquid/liquid interface *via* ion diffusion. $Cu(OH)_2$ was first formed after precipitation of Cu^{2+} and OH^-. The shape of $Cu(OH)_2$ was typical nanorods which was common in previous reports owing to the principal crystal structure of $Cu(OH)_2$.[18] The limited space probably forced the nanorods to aggregate together to reduce the surface energy of nanorods. Subsequently, the 3D nanorods further fused together in an interesting way. The nanorods attached each other parallelly, and formed nanosheets. The self-assembly of nanorods to generate nanosheets could be supported by the TEM image (Fig. 1d). At the edge of nanosheets, whisker like shape could be observed. The driving force is probably the high surface energy of nanorods as well as the narrow reaction space in which concentrated species are located. The nanosheets

retained the position and form 3D nanosheets. In the meantime, $Cu(OH)_2$ de-hydrated to generate CuO.

It has been reported that CuO can serve as an effective photocatalyst for the degradation of organic pollutants under visible light irradiation.[7c, d, 19] Herein, to qualitatively show the superiority of 3D macroporous CuO structures over non-organized nanosheets, commercial CuO or 3D structures composed by thicker sheets(Fig. S10), we investigated photocatalytic decomposition of rhodamine B (RhB) under visible light irradiation. Fig. 3a shows the time-dependent degradation curves of RhB in the presence of CuO catalysts after five times cycling. The degradation of RhB catalyzed by 3D macroporous CuO structures, non-organized nanosheets and 3D structures composed by thicker sheets were faster than commercial CuO, suggesting the nanosheets have higher catalytic activity. Better performance of 3D macroporous CuO structures than 3D structures composed by thicker sheets was observed, this could be attributed to the bigger surface area brought by the ultrathin nanosheets. Moreover, 3D macroporous CuO structures present an even higher efficiency than non-organized nanosheets during catalysis, which may come from the long term mesoscale structural stability of 3D macroporous CuO structures. Fig. 3b further confirms the long term catalytic activity of 3D nanosheets. The 3D macroporous CuO structures performed similar high activity during five times cycling test because the structures were maintained very well during cycling (Fig. S7). However, the activity of non-organized nanosheets decayed significantly during five times tests. SEM image of the samples taken after five times catalysis illustrated that non-organized nanosheets stack on each other (Fig. S8) (The non-organized nanosheets were well dispersed before catalysis (Fig. S9)). The reduced accessible surface of nanosheets is probably the reason that non-organized nanosheets performed worse than 3D nanosheets.

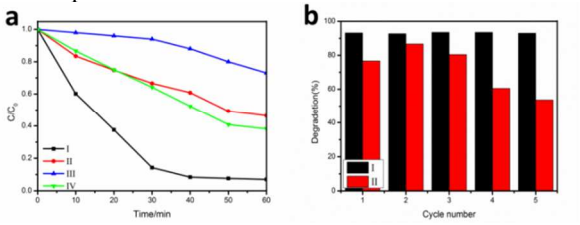

Fig. 3 (a) Time-dependent degradation curves of RhB catalyzed by 3D macroporous CuO structures constituted by ultrathin nanosheets(I), non-organized CuO nanosheets(II), commercial CuO powder(III) and 3D structures composed by thicker sheets (IV) at the fifth circle. (b) Long term catalytic activity of 3D macroporous CuO structures(I) and non-organized CuO nanosheets(II) in degrading RhB.

Not only in photocatalysis, the 3D macroporous CuO structures showed superior performance over 3D structures composed by thicker sheets, non-organized nanosheets and commercial CuO as the anode of lithium ion battery. The cycling performance and coulombic efficiency of the 3D macroporous CuO structures at a rate of 0.1 C are shown in Fig. 4. The capacity of 3D macroporous CuO structures can sustain 65% (390 $mAhg^{-1}$) capacity of the 2nd cycle (600 $mAhg^{-1}$) at a rate of 0.1 C after 30 cycles. The coulombic efficiency of the structures can sustain at about 100%. The relatively high reversible capacity could be attributed to its macroporous structure. The macroporous structure allows the nanosheets to interact with the electrolyte sufficiently, leading to a high discharging capacity. 3D structures composed by thicker sheets show lower capacity during cycling. The lower capacity of 3D CuO structures constituted of thick sheets could be attributed to the longer diffusion pathway perpendicular to the facet and smaller surface area. The non-organized nanosheets show even worse performance. The capacity reduced from 467 $mAhg^{-1}$ to 130 $mAhg^{-1}$, 72% percentage of capacity was lost. As the non-organized nanosheets would stack on each other easily, this could limit the chance of contact between electrolyte and the surface of material, further decrease the diffusion rate of ions in the battery. Commercial CuO shows lowest capacity because it processes no 3D structure or nanosheet when compared with the other samples. The stable cycling of commercial CuO probably comes from a better crystallinity. The XRD profiles of commercial CuO (Fig. S11) suggest that the crystallinity of commercial CuO is better that our 3D CuO because higher and narrower diffraction peaks with smaller full width at half maximum (FWHM) values were observed at ((11-1) and (111)) of commercial CuO.

In summary, we have proposed an approach to fabricate 3D macroporous CuO structures composed of ultrathin nanosheets by utilization of an interface between immiscible liquids. The confined reaction space facilitated the generation of ultrathin nanosheets, and made them assemble into a 3D macroporous structure. Such structure helped the nanosheets to keep exposed without stacking on each other during chemical reaction, and offered CuO superior long term activity both in photocatalysis and lithium ion battery. Such approach may open a general way to prepare 3D structures composed of ultrathin nanosheets, and provide superior catalyst or energy storage materials with long term activity.

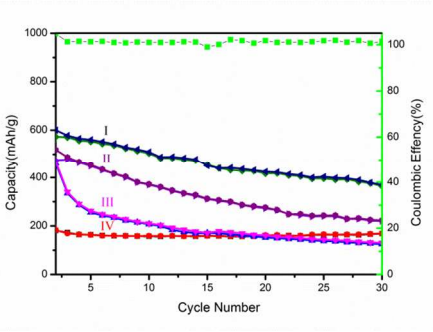

Fig. 4 Cycling performance of CuO samples. CuO structures constituted by ultrathin nanosheets(I), 3D structure with thick blocks(II), non-organized CuO nanosheets(III) and commercial CuO powder(IV). Coulombic efficiency of CuO structures constituted by ultrathin nanosheets is shown as the green line.

This work was supported by the National Natural Science Foundation of China (Grant No. 21173084) and the Large Instruments Open Foundation of East China Normal University.

Notes and references

[*a] Department of Physics, Center for Functional Nanomaterials and Devices,
East China Normal University, Shanghai, 200241, P.R. China.
E-mail: jsjiang@phy.ecnu.edu.cn
[b] Engineering Research Center of Advanced Glasses Manufacturing Technology, MOE, Donghua University, Shanghai 201620, P. R. China

† Electronic Supplementary Information (ESI) available: [XRD, FESEM pictures of the 3D macroporous CuO structures. FESEM images of the products obtained at different reaction times. TEM pictures of non-organized CuO nanosheets. The nitrogen adsorption–desorption isotherms of the 3D macroporous CuO structures.]. See DOI: 10.1039/c000000x/

1. (a) K. S. Novoselov, A. K. Geim, S. V. Morozov, D. Jiang, Y. Zhang, S. V. Dubonos, I. V. Grigorieva and A. A. Firsov, *Science*, 2004,

306, 666; (b) K. S. Novoselov, A. K. Geim, S. V. Morozov, D. Jiang, M. I. Katsnelson, I. V. Grigorieva, S. V. Dubonos and A. A. Firsov, *Nature*, 2005, **438**, 197.

2. (a) F. Zhang, C. Hou, Q. Zhang, H. Wang and Y. Li, *Mater. Chem. Phys.* , 2012, **135**, 826; (b) R. Wang, C. Xu, J. Sun, L. Gao and C. Lin, *J. Mater. Chem. A*, 2013, **1**, 1794; (c) M. Du, C. Xu, J. Sun and L. Gao, *Electrochim. Acta,* 2012, **80**, 302; (d) J. Chang, H. Xu, J. Sun and L. Gao, *J. Mater. Chem.* , 2012, **22**, 11146; (e) C. Xu, J. Sun and L. Gao, *Nanoscale*, 2012, **4**, 5425; (f) S. Ding, J. S. Chen, D. Luan, F. Y. Boey, S. Madhavi and X. W. Lou, *Chem. Commun.* , 2011, **47**, 5780; (g) S. Ding, D. Luan, F. Y. Boey, J. S. Chen and X. W. Lou, *Chem. Commun.* , 2011, **47**, 7155; (h) X. Wang, Y. Zhang, C. Zhi, X. Wang, D. Tang, Y. Xu, Q. Weng, X. Jiang, M. Mitome, D. Golberg and Y. Bando, *Nat. Commun.*, 2013, **4**, 2905; (i) Y. Zhang, K. Fugane, T. Mori, L. Niu and J. Ye, *J. Mater. Chem.* , 2012, **22**, 6575; (j) Y. Zhang, T. Mori, L. Niu and J. Ye, *Energy Environ. Sci.* , 2011, **4**, 4517.

3. (a) D. Ma, G. Shi, H. Wang, Q. Zhang and Y. Li, *Nanoscale*, 2013, **5**, 4808; (b) D. Ma, H. Wang, Q. Zhang and Y. Li, *J. Mater. Chem.* , 2012, **22**, 16633; (c) Q. Mu, Q. Zhang, H. Wang and Y. Li, *J. Mater. Chem.* , 2012, **22**, 16851; (d) D. Liu, X. Wang, X. Wang, W. Tian, J. Liu, C. Zhi, D. He, Y. Bando and D. Golberg, *J. Mater. Chem. A*, 2013, **1**, 1952; (e) A. Pakdel, X. Wang, C. Zhi, Y. Bando, K. Watanabe, T. Sekiguchi, T. Nakayama and D. Golberg, *J. Mater. Chem.* , 2012, **22**, 4818; (f) X. Wang, C. Zhi, L. Li, H. Zeng, C. Li, M. Mitome, D. Golberg and Y. Bando, *Adv. Mater.* , 2011, **23**, 4072; (g) C. Z. Yuan, L. Yang, L. R. Hou, L. F. Shen, X. G. Zhang and X. W. Lou, *Energy Environ. Sci.* , 2012, **5**, 7883; (h) S. H. Yang, X. F. Song, P. Zhang and L. Gao, *ACS Appl. Mat. Interfaces,* 2013, **5**, 3317; (i) Y. C. Jiang, S. D. Zhang, Q. Ji, J. Zhang, Z. P. Zhang and Z. Y. Wang, *J. Mater. Chem. A*, 2014, **2**, 4574; (j) M. Choi, K. Na, J. Kim, Y. Sakamoto, O. Terasaki and R. Ryoo, *Nature*, 2009, **461**, 246; (k) M. Hu, S. Ishihara and Y. Yamauchi, *Angew. Chem. Int. Ed.* , 2013, **52**, 1235.

4. (a) J. S. Chen, Y. L. Tan, C. M. Li, Y. L. Cheah, D. Luan, S. Madhavi, F. Y. C. Boey, L. A. Archer and X. W. Lou, *J. Am. Chem. Soc.* , 2010, **132**, 6124; (b) C. Hu, X. Zhang, W. T. Li, Y. Yan, G. C. Xi, H. F. Yang, J. F. Li and H. Bai, *J. Mater. Chem. A*, 2014, **2**, 2040.

5. (a) H. J. Zhang, Q. Q. He, F. J. Wei, Y. J. Tan, Y. Jiang, G. H. Zheng, G. J. Ding and Z. Jiao, *Mater. Lett.* , 2014, **120**, 200; (b) R. J. Wei, J. C. Hu, T. F. Zhou, X. L. Zhou, J. X. Liu and J. L. Li, *Acta Mater.* , 2014, **66**, 163; (c) Z. Sun, T. Liao, Y. Dou, S. M. Hwang, M. S. Park, L. Jiang, J. H. Kim and S. X. Dou, *Nat. Commun.*, 2014, **5**, 3813; (d) M. Chhowalla, H. S. Shin, G. Eda, L.-J. Li, K. P. Loh and H. Zhang, *Nat. Chem.*, 2013, **5**, 263.

6. (a) J. W. Sha, N. Q. Zhao, E. Z. Liu, C. S. Shi, C. N. He and J. J. Li, *Carbon*, 2014, **68**, 352; (b) Y. Zhao, K. Yao, Q. Cai, Z. J. Shi, M. Q. Sheng, H. Y. Lin and M. W. Shao, *CrystEngComm*, 2014, **16**, 270; (c) F.-Y. Su, C. You, Y.-B. He, W. Lv, W. Cui, F. Jin, B. Li, Q.-H. Yang and F. Kang, *J. Mater. Chem.* , 2010, **20**, 9644; (d) S. Ding, J. S. Chen, D. Luan, F. Y. C. Boey, S. Madhavi and X. W. Lou, *Chem. Commun.* , 2011, **47**, 5780; (e) D. Rangappa, K. D. Murukanahally, T. Tomai, A. Unemoto and I. Honma, *Nano Lett.* , 2012, **12**, 1146.

7. (a) L. Huang, F. Peng, H. Yu and H. Wang, *Solid State Sci.* , 2009, **11**, 129; (b) N. Mukherjee, B. Show, S. K. Maji, U. Madhu, S. K. Bhar, B. C. Mitra, G. G. Khan and A. Mondal, *Mater. Lett.* , 2011, **65**, 3248; (c) J. Liu, J. Jin, Z. Deng, S. Z. Huang, Z. Y. Hu, L. Wang, C. Wang, L. H. Chen, Y. Li, G. Van Tendeloo and B. L. Su, *J. Colloid Interface Sci.*, 2012, **384**, 1; (d) Y. Fan, R. Liu, W. Du, Q. Lu, H. Pang and F. Gao, *J. Mater. Chem.* , 2012, **22**, 12609.

8. P. Tian, X. Y. Han, G. L. Ning, H. X. Fang, J. W. Ye, W. T. Gong and Y. Lin, *ACS Appl. Mat. Interfaces,* 2013, **5**, 12411.

9. (a) X. Gou, G. Wang, J. Yang, J. Park and D. Wexler, *J. Mater. Chem.* , 2008, **18**, 965; (b) C. X. Wang, W. Zeng, H. Zhang, Y. Q. Li, W. G. Chen and Z. C. Wang, *J. Mater. Sci. - Mater. Electron.*, 2014, **25**, 2041; (c) R. K. Bedi and I. Singh, *ACS Appl. Mat. Interfaces,* 2010, **2**, 1361.

10. (a) J. Y. Xiang, J. P. Tu, L. Zhang, Y. Zhou, X. L. Wang and S. J. Shi, *J. Power Sources,* 2010, **195**, 313; (b) X. P. Gao, J. L. Bao, G. L. Pan, H. Y. Zhu, P. X. Huang, F. Wu and D. Y. Song, *J. Phys. Chem. B* 2004, **108**, 5547; (c) J. C. Park, J. Kim, H. Kwon and H. Song, *Adv. Mater.* , 2009, **21**, 803; (d) J. Wang, Y. Liu, S. Wang, X. Guo and Y. Liu, *J. Mater. Chem. A*, 2014, **2**, 1224; (e) S. Yuan, X. L. Huang, D. L. Ma, H. G. Wang, F. Z. Meng and X. B. Zhang, *Adv. Mater.* , 2014, **26**, 2273.

11. L. J. Wang, Q. Zhou, Y. J. Liang, H. L. Shi, G. L. Zhang, B. S. Wang, W. W. Zhang, B. Lei and W. Z. Wang, *Appl. Surf. Sci.* , 2013, **271**, 136.

12. (a) Y. Liu, W. Wang, L. Gu, Y. Wang, Y. Ying, Y. Mao, L. Sun and X. Peng, *ACS Appl. Mat. Interfaces,* 2013, **5**, 9850; (b) X. Chen, N. Zhang and K. Sun, *J. Mater. Chem.* , 2012, **22**, 13637.

13. (a) M. A. Worsley, T. Y. Olson, J. R. I. Lee, T. M. Willey, M. H. Nielsen, S. K. Roberts, P. J. Pauzauskie, J. Biener, J. H. Satcher and T. F. Baumann, *J. Phys. Chem. Lett.* , 2011, **2**, 921; (b) Z. Chen, W. Ren, L. Gao, B. Liu, S. Pei and H.-M. Cheng, *Nat. Mater.* , 2011, **10**, 424; (c) G. L. Wang, J. C. Huang, S. L. Chen, Y. Y. Gao and D. X. Cao, *J. Power Sources,* 2011, **196**, 5756; (d) L. Liu, Y. Li, S. Yuan, M. Ge, M. Ren, C. Sun and Z. Zhou, *J. Phys. Chem. C* 2010, **114**, 251.

14. Y. K. Yin, Y. L. Xu, Y. Li, F. Y. Ren, S. J. Li, G. Jin, M. J. Li and X. Y. Cui, *Chem. Res. Chin. Univ.* , 2013, **29**, 379.

15. L. j. FU Dong, LIU jinchen, and LI yigui, *J. Chem. Ind. Eng.*, 2002, **53**, 7.

16. Weil, K. G. (1984), J. S. Rowlinson and B. Widom: Molecular Theory of Capillarity, Clarendon Press, Oxford 1982. 327.

17. (a) J. Zhu and X. Qian, *J. Solid State Chem.* , 2010, **183**, 1632; (b) Z. H. Ibupoto, K. Khun, V. Beni, X. Liu and M. Willander, *Sensors*, 2013, **13**, 7926; (c) Y. Xu, D. Chen, X. Jiao and K. Xue, *Mater. Res. Bull.* , 2007, **42**, 1723; (d) L. Zheng and X. Liu, *Mater. Lett.* , 2007, **61**, 2222; (e) J. G. Zhao, S. J. Liu, S. H. Yang and S. G. Yang, *Appl. Surf. Sci.* , 2011, **257**, 9678; (f) M. Faisal, S. B. Khan, M. M. Rahman, A. Jamal and A. Umar, *Mater. Lett.* , 2011, **65**, 1400; (g) F. Li, X. Liu, Q. Zhang, T. Kong and H. Jin, *Cryst. Res. Technol.* , 2012, **47**, 1140.

18. (a) X. G. Wen, W. X. Zhang and S. H. Yang, *Langmuir*, 2003, **19**, 5898; (b) C. H. Lu, L. M. Qi, J. H. Yang, D. Y. Zhang, N. Z. Wu and J. M. Ma, *J. Phys. Chem. B* 2004, **108**, 17825.

19. S. P. Meshram, P. V. Adhyapak, U. P. Mulik and D. P. Amalnerkar, *Chem. Eng. J.* , 2012, **204-206**, 158.

